LETTER

Direct measurement of the quantum wavefunction

Jeff S. Lundeen[1], Brandon Sutherland[1], Aabid Patel[1], Corey Stewart[1] & Charles Bamber[1]

The wavefunction is the complex distribution used to completely describe a quantum system, and is central to quantum theory. But despite its fundamental role, it is typically introduced as an abstract element of the theory with no explicit definition[1,2]. Rather, physicists come to a working understanding of the wavefunction through its use to calculate measurement outcome probabilities by way of the Born rule[3]. At present, the wavefunction is determined through tomographic methods[4–8], which estimate the wavefunction most consistent with a diverse collection of measurements. The indirectness of these methods compounds the problem of defining the wavefunction. Here we show that the wavefunction can be measured directly by the sequential measurement of two complementary variables of the system. The crux of our method is that the first measurement is performed in a gentle way through weak measurement[9–18], so as not to invalidate the second. The result is that the real and imaginary components of the wavefunction appear directly on our measurement apparatus. We give an experimental example by directly measuring the transverse spatial wavefunction of a single photon, a task not previously realized by any method. We show that the concept is universal, being applicable to other degrees of freedom of the photon, such as polarization or frequency, and to other quantum systems—for example, electron spins, SQUIDs (superconducting quantum interference devices) and trapped ions. Consequently, this method gives the wavefunction a straightforward and general definition in terms of a specific set of experimental operations[19]. We expect it to expand the range of quantum systems that can be characterized and to initiate new avenues in fundamental quantum theory.

The wavefunction Ψ, also known as the 'quantum state', is considerably more difficult to measure than the state of a classical particle, which is determined simply by measuring its position X and momentum P. According to the Heisenberg uncertainty principle, in quantum theory a precise measurement of X disturbs the particle's wavefunction and forces a subsequent measurement of P to become random. Thus we learn nothing of the particle's momentum. Indeed, it is impossible to determine a completely unknown wavefunction of single system[20].

Consider instead performing a measurement of X on an ensemble of particles, all with the same Ψ. The probability of getting result $X = x$ is $|\Psi(x)|^2$. Similarly, the probability of $P = p$ would be $|\Phi(p)|^2$, where $\Phi(p)$ is the Fourier transform of $\Psi(x)$. Even these two probability distributions are not enough to determine $\Psi(x)$ unambiguously (see the one-dimensional phase retrieval problem[21]). Instead, Ψ must be reconstructed by performing a large set of distinct measurements (for example, of quadratures $Q(\theta) = X\cos(\theta) + P\sin(\theta)$, for mixing angles, θ, ranging from 0 to 2π), and then estimating a Ψ that is most compatible with the measurement results. This method is known as quantum state tomography[4–8]. In contrast, we introduce a method to measure Ψ of an ensemble directly. By 'direct' we mean that the method is free from complicated sets of measurements and computations; the average raw signal originating from where the wavefunction is being probed is simply proportional to its real and imaginary components at that point. The method rests on the sequential measurement of two complementary variables of the system.

At the centre of the direct measurement method is a reduction of the disturbance induced by the first measurement. Consider the measurement of an arbitrary variable A. In general, measurement can be seen as the coupling between an apparatus and a physical system that results in the translation of a pointer. The pointer position indicates the result of a measurement. In a technique known as 'weak measurement', the coupling strength is reduced and this correspondingly reduces the disturbance created by the measurement[9–18]. This strategy also compromises measurement precision, but this can be regained by averaging. The average of the weak measurement is simply the expectation value $\langle\Psi|A|\Psi\rangle$, indicated by an average position shift of the pointer proportional to this amount.

A distinguishing feature of weak measurement is that it does not disturb a subsequent normal (or 'strong') measurement of another observable C in the limit where the coupling vanishes. For the particular ensemble subset that gave outcome $C = c$, one can derive the average of the weak measurement of A. In the limit of zero interaction strength, this is called the 'weak value' and is given[9] by:

$$\langle A\rangle_W = \frac{\langle c|A|\Psi\rangle}{\langle c|\Psi\rangle} \tag{1}$$

Selecting a particular subset of an ensemble based on a subsequent measurement outcome is known as 'post-selection', and is a common tool in quantum information processing[22,23].

Unlike the standard expectation value $\langle A\rangle$, the weak value $\langle A\rangle_W$ can be a complex number. This seemingly strange result can be shown to have a simple physical manifestation: the pointer's position is shifted by $\mathrm{Re}\langle A\rangle_W$ and receives a momentum kick of $\mathrm{Im}\langle A\rangle_W$ (refs 24–26). The complex nature of the weak value suggests that it could be used to indicate both the real and the imaginary parts of the wavefunction.

Returning to our example of a single particle, consider the weak measurement of position ($A = \pi_x \equiv |x\rangle\langle x|$) followed by a strong measurement of momentum giving $P = p$. In this case, the weak value is:

$$\langle\pi_x\rangle_W = \frac{\langle p|x\rangle\langle x|\Psi\rangle}{\langle p|\Psi\rangle} \tag{2}$$

$$= \frac{e^{ipx/\hbar}\Psi(x)}{\Phi(p)} \tag{3}$$

In the case $p = 0$, this simplifies to

$$\langle\pi_x\rangle_W = k\Psi(x) \tag{4}$$

where $k = 1/\Phi(0)$ is a constant (which can be eliminated later by normalizing the wavefunction). The average result of the weak measurement of π_x is proportional to the wavefunction of the particle at x. Scanning the weak measurement through x gives the complete wavefunction. At each x, the observed position and momentum shifts of the measurement pointer are proportional to $\mathrm{Re}\Psi(x)$ and $\mathrm{Im}\Psi(x)$, respectively. In short, by reducing the disturbance induced by measuring X and then measuring P normally, we measure the wavefunction of the single particle.

As an experimental example, we performed a direct measurement of the transverse spatial wavefunction of a photon. Considering a photon travelling along the z direction, we directly measure the x wavefunction

[1]Institute for National Measurement Standards, National Research Council, 1200 Montreal Road, Ottawa, Canada, K1A 0R6.

of the photon, sometimes called the 'spatial mode' (see Supplementary Discussion). The Wigner function of the spatial mode of a classical beam has been measured directly but not for a single photon state[27,28].

We produce a stream of photons in one of two ways, either by attenuating a laser beam or by generating single photons through spontaneous parametric down-conversion (SPDC; see Supplementary Methods for details). The photons have a centre wavelength of $\lambda = 783$ nm or 800 nm, respectively. The experiment (details and diagram in Fig. 1) can be divided into four sequential steps: preparation of the transverse wavefunction, weak measurement of the transverse position of the photon, post-selection of those photons with zero transverse momenta, and readout of the weak measurement.

An ensemble of photons with wavefunction $\Psi(x)$ is emitted from a single mode fibre and collimated. We begin by directly measuring this wavefunction (described in detail in Fig. 1). We then further test our method by inducing known magnitude and phase changes to the photons here to prepare a series of modified wavefunctions.

We weakly measure the transverse position of the photon by coupling it to an internal degree of freedom of the photon, its polarization. This allows us to use the linear polarization angle of the photon as the pointer. At a position x where we wish to measure $\pi_x = |x\rangle\langle x|$, we rotate the linear polarization of the light by α. Consider if α is set to 90°. In this case, one can perfectly discriminate whether a photon had position x because it is possible to perfectly discriminate between orthogonal polarizations, 0° and 90°. This is a strong measurement. Reducing the strength of the measurement corresponds to reducing α, which makes it impossible to discriminate with certainty whether any

particular photon had $X = x$. The benefit of this reduction in precision is a commensurate reduction in the disturbance to the wavefunction of the single photon.

We then use a Fourier transform lens and a slit to post-select only those photons with $p = 0$. This constitutes the strong measurement of P.

In this subset of the photon ensemble, we find the average value of our weak measurement of π_x. The average rotation of the pointer, the linear polarization, is proportional to the real part of the weak value. Its complementary pointer variable, the rotation in the circular polarization basis, is proportional to the imaginary part of the weak value[25]. Formally, if we treat the initial polarization as a spin-1/2 spin-down vector, then the weak value is given by

$$\langle\pi_x\rangle_W = \frac{1}{\sin\alpha}\left(\langle s|\sigma_x|\rangle s - i\langle s|\sigma_y|s\rangle\right) \qquad (5)$$

where σ_x and σ_y are the Pauli x and y matrices, respectively, and $|s\rangle$ is the final polarization state of the pointer[25]. We measure the σ_x and σ_y expectation values by sending the photons through a half-wave plate or a quarter-wave plate, respectively, and then through a polarizing beamsplitter (PBS). Thus, we read out $\mathrm{Re}\Psi(x)$ (half-wave plate) and $\mathrm{Im}\Psi(x)$ (quarter-wave plate) from the signal imbalance between detectors 1 and 2 at the outputs of the PBS (Fig. 1).

With $\alpha = 20°$, we scan our measurement of π_x in 1-mm steps and find the weak value $\langle\pi_x\rangle_W$ at each step. In this way, we directly measure the photon transverse wavefunction, $\Psi(x) = |\Psi(x)|\exp(i\phi(x))$. We normalize the σ_x and σ_y measurements by the same factor, so that $\int|\Psi(x)|^2 dx = 1$, which eliminates the proportionality constant, $\sin\alpha/\Phi(0)$.

To confirm our direct measurement method, we test it on a series of different wavefunctions. Using our SPDC single photon source, we start by measuring the initial truncated Gaussian wavefunction (Fig. 2) described in Fig. 1. Switching to the laser source of photons, we then modify the magnitude, and then the phase, of the initial wavefunction with an apodized filter and glass plate, respectively, to create two new test Ψ (Fig. 3). We conduct more quantitative modification of the wavefunction phase by introducing a series of phase gradients and then phase curvatures (Fig. 4). For all the test wavefunctions, we have found
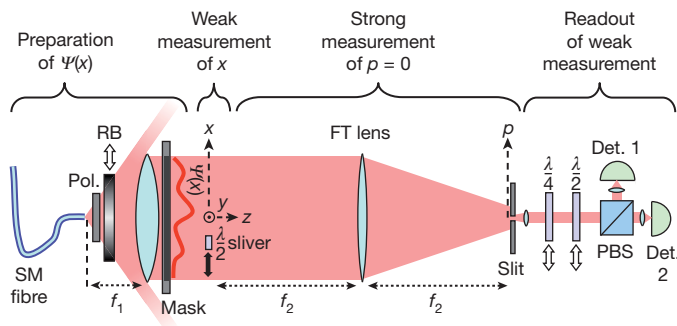

Figure 1 | Direct measurement of the photon transverse wavefunction. To begin with photons having identical wavefunctions, we transmit them through an optical fibre (Nufern PM780-HP) that allows only a single mode (SM) to pass. This mode is approximately Gaussian, with a nominal $1/e^2$ diameter of 5.3 ± 1.0 μm. The photons emerge from the fibre and pass through a micro-wire polarizer (Pol.; Edmund Optic NT47-602) to be collimated by an achromatic lens ($f_1 = 30$ cm, diameter 5 cm, Thorlabs AC508-300-B), one focal length (f_1) away from the fibre. The lens was masked off with a rectangular aperture of dimension $x \times y = 43$ mm $\times$ 11 mm. Thus our nominal initial wavefunction was a truncated Gaussian with a $1/e^2$ diameter of 56.4 mm and a flat phase profile. We modify the magnitude and phase of the nominal $\Psi(x)$ to create a series of test wavefunctions (see Figs 3, 4). At 45 mm past the lens, a rectangular sliver of a half-wave plate ($\lambda/2$ sliver) ($x \times y \times z$ dimensions of 1 mm $\times$ 25 mm $\times$ 1 mm) at position x is used to weakly measure $\pi_x = |x\rangle\langle x|$ (see Supplementary Methods for details). The photons then undergo an optical Fourier transform (FT) induced by an achromatic lens ($f_2 = 1$ m, diameter 5 cm, Thorlabs AC508-1000-B), placed one focal length (f_2) from the waveplate sliver. In the Fourier transform plane, one focal length f_2 past the lens, we post-select those photons with $p = 0$ by accepting only those that pass through a 15-μm-wide slit on axis. We collimate the photons emerging from the slit with an $f_3 = 3$ cm focal length lens. The photons pass through either a half-wave plate ($\lambda/2$) or quarter-wave plate ($\lambda/4$) and then through a polarizing beamsplitter (PBS). At each output port, the photons are focused onto a detector (Det. 1 and Det. 2): for the single photons, a photon counter (silicon avalanche photodiodes, PerkinElmer SPCM-AQHR-14); and for the laser, a silicon photodiode (Thorlabs, DET10A). The imbalance in counts or signal between the two detectors is proportional to the real ($\lambda/2$) or imaginary ($\lambda/4$) part of the wavefunction.
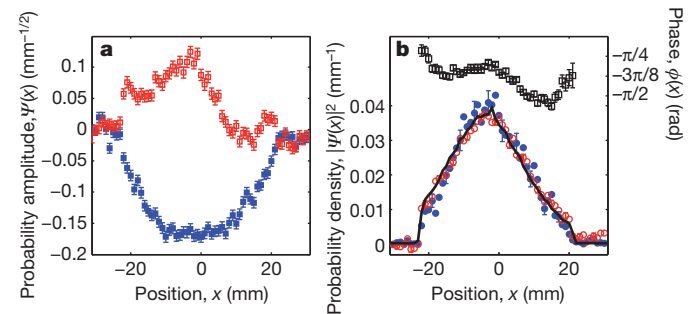

Figure 2 | The measured single-photon wavefunction, $\Psi(x)$, and its modulus squared and phase. a, $\mathrm{Re}\Psi(x)$ (solid blue squares) and $\mathrm{Im}\Psi(x)$ (open red squares) measured for the truncated Gaussian wavefunction. **b,** Using the data in **a** we plot the phase $\phi(x) = \arctan(\mathrm{Re}\Psi(x)/\mathrm{Im}\Psi(x))$ (open squares; right axis) and the modulus squared $|\Psi(x)|^2$ (solid blue circles; left axis). There is good agreement between the latter and a strong measurement of the x probability distribution Prob(x) (solid line; left axis) conducted by scanning a detector along x in the plane of the sliver. The phase is relatively flat, as expected from the fibre mode. The slight variation is consistent with the manufacturer specification of the first lens and the phase curvature measured with a shear plate. We also removed the slit completely. In this case, there is no post-selection and the weak value $\langle\pi_x\rangle$ becomes equal to the standard expectation value $\langle\Psi|\pi_x|\Psi\rangle = |\Psi(x)|^2$. We plot the measured $\mathrm{Re}\langle\pi_x\rangle$ (open red circles; left axis) after it is normalized so that $\int \mathrm{Re}\,\Psi(x)dx = 1$ and find it is in good agreement with Prob(x). We find that $\mathrm{Im}\langle\pi_x\rangle$ is ten times smaller, making $\langle\pi_x\rangle$ largely real, as expected. Error bars are ± 1 s.d. found from statistics in repeated scans. In **b**, only every third error bar is shown for clarity.
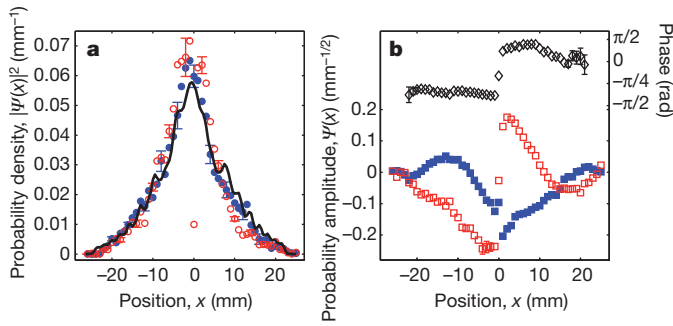
Figure 3 | Measurements of modified wavefunctions. We further test our ability to measure $\Psi(x)$ by changing $\mathrm{Prob}(x)$ by placing a reverse bull's-eye spatially apodized attenuator (RB in Fig. 1) (Edmund Optics, NT64-388) after the fibre. **a**, We calculate $|\Psi(x)|^2$ from the data (solid blue circles) along with a detector scan of $\mathrm{Prob}(x)$ (solid line) and find good agreement between the two. **b**, With the reverse bull's eye still in place, we modify the phase profile $\phi(x)$ of the wavefunction by creating a phase discontinuity at $x = 0$ imposed with a glass plate half-way across $\Psi(x)$. At the bottom, we show $\mathrm{Re}\Psi(x)$ (solid blue squares; left axis) and $\mathrm{Im}\Psi(x)$ (open red squares; left axis), which exhibit a discontinuity at the plate edge. This discontinuity is even clearer in the phase difference between the wavefunctions measured with and without the glass plate, shown at the top (open black diamonds; right axis). Despite their discontinuities, if we use $\mathrm{Re}\Psi(x)$ and $\mathrm{Im}\Psi(x)$ to calculate $|\Psi(x)|^2$ (open red circles in **a**), we find that it is largely unchanged by the glass plate. This is as expected, as the glass has a transmission near unity. Error bars are ± 1 s.d. found from statistics in repeated scans. In **a**, every third error bar is shown for clarity. In **b**, those bars smaller than the symbols are not shown.

Figure 4 | Phase modification of the wavefunction. a, We displace the slit transversely by $\Delta x_{\mathrm{slit}} = -30, -20, -10, 10, 20, 30$ and $40\,\mu\mathrm{m}$ (curves in main panel, top to bottom). This effectively redefines the zero momentum axis of the system. Our photons now travel at an angle to this axis or equivalently the wavefunction has a linear phase gradient, $\phi(x) = mx$, where $m = \Delta x_{\mathrm{slit}} 2\pi/f_2\lambda$. We plot the phase difference between the original wavefunction and those with a phase gradient. For clarity, the curves have been offset to cross at $-20\,\mathrm{mm}$. This corresponds to shifting the arbitrary global phase of $\Psi(x)$. Inset, gradient m as a function of Δx_{slit} (circles) along with theory (line), which show good agreement. **b**, We introduce a quadratic phase by displacing the first lens by $\Delta z = 200, 400, 600$ and $800\,\mu\mathrm{m}$ (curves in main panel, bottom to top) along with theoretical fits (lines). The phase $\phi(x) = rx^2$, where the phase curvature $r = \pi\Delta z/f_1^2\lambda$. Inset, the phase curvature r from these fits (circles) as a function of lens displacement, Δx_{slit}, which shows good agreement with theory (line). Statistical error bars (± 1 s.d.) are smaller than the symbols in all plots.

good agreement between the expected and measured wavefunction, including its phase and magnitude (see the figure legends for details).

We now describe how the technique of weak measurement can be used to directly measure the quantum state of an arbitrary quantum system. We have the freedom to measure the quantum state in any chosen basis $\{|a\rangle\}$ (associated with observable A) of the system. The method entails weakly measuring a projector in this basis, $\pi_a \equiv |a\rangle\langle a|$, and post-selecting on a particular value b_0 of the complementary observable B (see Supplementary Discussion for a precise definition of complementarity). In this case, the weak value is

$$\langle \pi_a \rangle_{\mathrm{W}} = \frac{\langle b_0|a\rangle\,\langle a|\Psi\rangle}{\langle b_0|\Psi\rangle} = \langle a|\Psi\rangle/\nu \qquad (6)$$

where ν is a constant, independent of a. Thus the weak value is proportional to the amplitude of state $|a\rangle$ in the quantum state. Stepping a through all the states in the A basis directly gives the quantum state represented in that basis:

$$|\Psi\rangle = \nu \sum_a \langle \pi_a \rangle_{\mathrm{W}}|a\rangle \qquad (7)$$

This is the general theoretical result of this Letter. It shows that in any physical system one can directly measure the quantum state of that system by scanning a weak measurement through a basis and appropriately post-selecting in the complementary basis.

Weak measurement necessarily trades efficiency for accuracy or precision. A comparison of our method to current tomographic reconstruction techniques will require careful consideration of the signal to noise ratio in a given system. In order to increase this ratio in the direct measurement of the photon spatial wavefunction, future experiments will investigate the simultaneous post-selection of many transverse momenta.

In our direct measurement method, the wavefunction manifests itself as shifts of the pointer of the measurement apparatus. In this sense, the method provides a simple and unambiguous operational definition[19] of the quantum state: it is the average result of a weak measurement of a variable followed by a strong measurement of the complementary variable. We anticipate that the simplicity of the method will make feasible the measurement of quantum systems
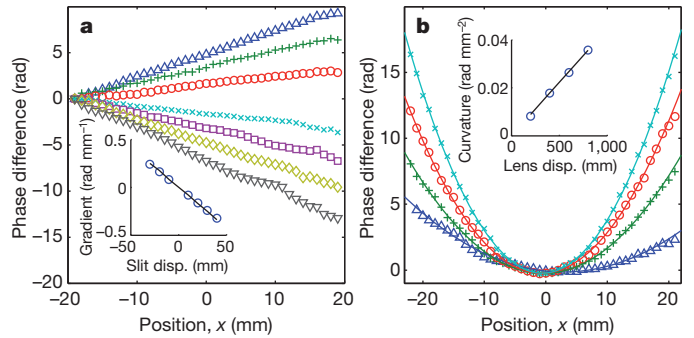
(for example, atomic orbitals, molecular wavefunctions[29], ultrafast quantum wavepackets[30]) that previously could not be fully characterized. The method can also be viewed as a transcription of quantum state of the system to that of the pointer, a potentially useful protocol for quantum information.

1. Cohen-Tannoudji, C., Diu, B. & Laloe, F. *Quantum Mechanics* Vol. 1, 19 (Wiley-Interscience, 2006).
2. Mermin, N. D. What's bad about this habit. *Phys. Today* **62**, 8–9 (2009).
3. Landau, L. D. & Lifshitz, E. M. *Course of Theoretical Physics* Vol. 3, *Quantum Mechanics: Non-Relativistic Theory* 3rd edn, 6 (Pergamon, 1989).
4. Vogel, K. & Risken, H. Determination of quasiprobability distributions in terms of probability distributions for the rotated quadrature phase. *Phys. Rev. A* **40**, 2847–2849 (1989).
5. Smithey, D. T., Beck, M., Raymer, M. G. & Faridani, A. Measurement of the Wigner distribution and the density matrix of a light mode using optical homodyne tomography: application to squeezed states and the vacuum. *Phys. Rev. Lett.* **70**, 1244–1247 (1993).
6. Breitenbach, G., Schiller, S. & Mlynek, J. Measurement of the quantum states of squeezed light. *Nature* **387**, 471–475 (1997).
7. White, A. G., James, D. F. V., Eberhard, P. H. & Kwiat, P. G. Nonmaximally entangled states: production, characterization, and utilization. *Phys. Rev. Lett.* **83**, 3103–3107 (1999).
8. Hofheinz, M. *et al.* Synthesizing arbitrary quantum states in a superconducting resonator. *Nature* **459**, 546–549 (2009).
9. Aharonov, Y., Albert, D. Z. & Vaidman, L. How the result of a measurement of a component of the spin of a spin-1/2 particle can turn out to be 100. *Phys. Rev. Lett.* **60**, 1351–1354 (1988).
10. Ritchie, N. W. M., Story, J. G. & Hulet, R. G. Realization of a measurement of a "weak value". *Phys. Rev. Lett.* **66**, 1107–1110 (1991).
11. Resch, K. J., Lundeen, J. S. & Steinberg, A. M. Experimental realization of the quantum box problem. *Phys. Lett. A* **324**, 125–131 (2004).
12. Smith, G. A., Chaudhury, S., Silberfarb, A., Deutsch, I. H. & Jessen, P. S. Continuous weak measurement and nonlinear dynamics in a cold spin ensemble. *Phys. Rev. Lett.* **93**, 163602 (2004).
13. Pryde, G. J., O'Brien, J. L., White, A. G., Ralph, T. C. & Wiseman, H. M. Measurement of quantum weak values of photon polarization. *Phys. Rev. Lett.* **94**, 220405 (2005).
14. Mir, R. *et al.* A double-slit 'which-way' experiment on the complementarity-uncertainty debate. *N. J. Phys.* **9**, 287 (2007).
15. Hosten, O. & Kwiat, P. Observation of the spin Hall effect of light via weak measurements. *Science* **319**, 787–790 (2008).
16. Dixon, P. B., Starling, D. J., Jordan, A. N. & Howell, J. C. Ultrasensitive beam deflection measurement via interferometric weak value amplification. *Phys. Rev. Lett.* **102**, 173601 (2009).
17. Lundeen, J. S. & Steinberg, A. M. Experimental joint weak measurement on a photon pair as a probe of Hardy's paradox. *Phys. Rev. Lett.* **102**, 020404 (2009).

18. Aharonov, Y., Popescu, S. & Tollaksen, J. A time-symmetric formulation of quantum mechanics. *Phys. Today* **63,** 27–32 (2010).
19. Bridgman, P. *The Logic of Modern Physics* (Macmillan, 1927).
20. Wootters, W. K. & Zurek, W. H. A single quantum cannot be cloned. *Nature* **299,** 802–803 (1982).
21. Trebino, R. *Frequency-Resolved Optical Gating: The Measurement of Ultrashort Laser Pulses* (Springer, 2002).
22. Knill, E., Laflamme, R. & Milburn, G. J. A scheme for efficient quantum computation with linear optics. *Nature* **409,** 46–52 (2001).
23. Duan, L. M., Lukin, M. D., Cirac, J. I. & Zoller, P. Long-distance quantum communication with atomic ensembles and linear optics. *Nature* **414,** 413–418 (2001).
24. Aharonov, Y. & Vaidman, L. Properties of a quantum system during the time interval between two measurements. *Phys. Rev. A* **41,** 11–20 (1990).
25. Lundeen, J. S. & Resch, K. J. Practical measurement of joint weak values and their connection to the annihilation operator. *Phys. Lett. A* **334,** 337–344 (2005).
26. Jozsa, R. Complex weak values in quantum measurement. *Phys. Rev. A* **76,** 044103 (2007).
27. Mukamel, E., Banaszek, K., Walmsley, I. A. & Dorrer, C. Direct measurement of the spatial Wigner function with area-integrated detection. *Opt. Lett.* **28,** 1317–1319 (2003).
28. Smith, B. J., Killett, B., Raymer, M. G., Walmsley, I. A. & Banaszek, K. Measurement of the transverse spatial quantum state of light at the single-photon level. *Opt. Lett.* **30,** 3365–3367 (2005).
29. Itatani, J. *et al.* Tomographic imaging of molecular orbitals. *Nature* **432,** 867–871 (2004).
30. Dudovich, N. *et al.* Measuring and controlling the birth of attosecond XUV pulses. *Nature Phys.* **2,** 781–786 (2006).

Supplementary Information is linked to the online version of the paper at www.nature.com/nature.

Author Information Reprints and permissions information is available at www.nature.com/reprints. The authors declare no competing financial interests. Readers are welcome to comment on the online version of this article at www.nature.com/nature. Correspondence and requests for materials should be addressed to J.S.L. (jeff.lundeen@nrc-cnrc.gc.ca).